

Wave merging mechanism: formation of low-frequency Alfvén and magnetosonic waves in cosmic plasmas

V.N. Tishchenko, I.F. Shaikhislamov

Abstract. We investigate the merging mechanism for the waves produced by a pulsating cosmic plasma source. A model with a separate background/source description is used in our calculations. The mechanism was shown to operate both for strong and weak source–background interactions. We revealed the effect of merging of individual Alfvén waves into a narrow low-frequency wave, whose amplitude is maximal for a plasma expansion velocity equal to 0.5–1 of the Alfvén Mach number. This wave is followed along the field by a narrow low-frequency magnetosonic wave, which contains the bulk of source energy. For low expansion velocities the wave contains background and source particles, but for high velocities it contains only the background particles. The wave lengths are much greater than their transverse dimension.

Keywords: wave merging mechanism, pulsating plasma, magnetic field, Alfvén wave, magnetosonic wave.

The shock-wave merging mechanism (SWMM) was proposed and experimentally confirmed for optical pulsed discharges produced by repetitively pulsed laser radiation in gases [1–4]. The SWMM is efficient for the formation of low-frequency quasi-stationary waves (QWs), whose length depends linearly on the number of pulses and the energy expended for its production. For single optical breakdowns or explosions the lengths of shock waves depend only slightly on the pulse energy ($\propto Q^{1/6}$).

The present work (like Refs [5, 6]) was performed in the framework of the hypothesis that the SWMM is universal in character and is operative in different media and for different sources of natural or artificial origin. This is suggested by the kind of SWMM criteria: the initial wave velocity is higher than the sound velocity in the medium (hereinafter referred to as the background); optimal frequencies $\Delta\omega$ (dimensionless) depend on the geometry of QW propagation. The high efficiency of source-to-QW energy conversion is attainable when additional background-dependent conditions are fulfilled. The following conditions must be fulfilled in a rarefied plasma with magnetic field: the initial pressure in the source is much higher than the combined pressure of the magnetic field and the background plasma; the source plasma is completely ionised and, as shown in this work (see below), the initial plasma

velocity amounts to ~ 0.5 –1 of the Alfvén wave velocity in the background. These conditions may be attained with the use of a laser plasma produced by repetitively pulsed laser radiation on the surface of a solid. Laser sources permit controlling the duration of a QW and its spectrum by varying the number of pulses and their repetition rate. The pulse duration must be much shorter than the plasma expansion time (~ 1 μ s) [2] and the pulse energy density at the surface must be several times higher than the optical breakdown threshold.

Different types of waves are possible in cosmic plasmas with magnetic field [7, 8]. If the hypothesis under discussion is correct, one would expect the formation of the corresponding QWs, including magnetosonic, Alfvén, and whistler waves. A cylindrical source parallel to the magnetic field forms a fast magnetosonic QW (MQW) propagating transversely to the field [5]. A point source produces a so-called narrow slow MQW, which travels along the magnetic field [6]. For a magnetised background, in which the thermal pressure of the plasma with electron and ion densities n_e and n_i is much lower than the pressure of the magnetic field of intensity B_0 ,

$$\beta \ll k_B T_0 (n_i + n_e) / (B_0^2 / 8\pi) \ll 1,$$

the MQW velocity is close to the ion-sound velocity [6]. The MQW length depends linearly on the number of pulses and its transverse dimension is approximately equal to the dynamic radius R_d of a single pulse. For a large number of pulses the MQW length is far greater than R_d , and this wave is therefore referred to as a narrow MQW. The radial MQW expansion is hindered by the magnetic field. In Ref. [6] we considered a one-fluid magnetohydrodynamic (MHD) model, which corresponds to the case of a short (in comparison with R_d) ion Larmor gyration radius R_L in magnetic field and interaction of strong source ions with background.

In the present work, the SWMM was investigated for the conditions whereby the ion plasma length L_{pi} as well as R_L are much longer than R_d , which corresponds to electrodynamic, or weak, source plasma–background interaction. Narrow Alfvén QWs (AQWs) and MQWs were considered. In simulations on a cluster, use was made of a three-fluid MHD model in the two-dimensional cylindrical geometry with axial symmetry. The first fluid describes the background ions, the second fluid describes the source ions and the third one – the electrons, which are common for the background and the source: $n_e = z_0 n_0 + z_q n_q$ (z_0 and z_q are the ion charges). Account was taken of thermal pressure forces, the magnetic force and cohesion of the fluids via the Lorentz force in the motion of the plasmas (magnetic laminar mechanism). Electromagnetic fields were determined from Maxwell’s equation. We con-

V.N. Tishchenko, I.F. Shaikhislamov Institute of Laser Physics, Siberian Branch, Russian Academy of Sciences, prosp. Akad. Lavrent’eva 13/3, 630090 Novosibirsk, Russia; e-mail: tvn25@ngs.ru, ildars@ngs.ru

Received 15 October 2013; revision received 21 December 2013
Kvantovaya Elektronika 44 (2) 98–101 (2014)
Translated by E.N. Ragozin

sidered an infinite volume of a uniform, collisionless, quasi-neutral, fully ionised ideal plasma with a density n_0 , temperature T_0 , and uniform magnetic field B_0 . The ion charge and mass are $z_0 = 1$ and $m_0 = 1$; we selected $\beta = 0.006$, which is close to the parameters of the interplanetary medium in the solar system. At a point ($r = 0, z = 0$) there occur periodic ejections of a hot plasma with a repetition rate f . Each ejection is confined within a spherical volume $R_Q \sim 0.2R_d$, has an energy Q and a mass M for an ion mass and charge m_q and z_q . We varied the pulse repetition rate, the number of pulses, and the ion expansion velocity V_0 , which changed in relation to their number.

The SWMM forms a QW for a certain relation between Q, f , and the wave velocity C_i in the background. Like in gases [1, 2], for an immobile source the wave formation criterion is of the form

$$\omega_i = fR_d/C_i.$$

Here C_i is the Alfvén (C_A) or magnetosonic (C_s) wave velocity. To describe the AQW, use was made of the Mach number $M_A = V_0/C_A$, the time was normalised to a quantity R_d/C_A and the frequency to its inverse quantity; for the MQW, use was made of the Mach number $M_s = V_0/C_s$ and the time was normalised to R_d/C_s . Spatial variables were normalised to $R_d = \{Q/[B_0^2/8\pi + k_B T_0(n_i + n_e)]\}^{1/3}$. The SWMM universality implies that the SWMM operates in different media in the same frequency range $\Delta\omega$, which depends on the wave expansion geometry. In gases there are domains bounded by frequencies $\omega_1, \omega_2, \omega_3$. For $\omega < \omega_1$ the shock waves propagate independently; in the $\omega_1 < \omega < \omega_2$ domain their interaction strengthens with increasing ω ; for $\omega_2 < \omega < \omega_3$ the compression phases of the shock waves partly overlap to form a QW. When $\omega > 2\omega_2$, the length of the common wave depends only slightly on the total energy. For a spherical expansion $\omega_1 \sim 0.8$ and $\omega_2 \sim 5.6$, while for a one-dimensional expansion $\omega_1 \sim 0.1$ and $\omega_2 \sim 1$.

Since Alfvén and magnetosonic waves propagate one-dimensionally [6–8], AQWs and MQWs would be expected in the frequency range $\omega \sim 0.1–1$. Figure 1 shows the variation of MQW structure with ω and t . The source is located at a point $z = 0, r = 0$, the z MQW axis is aligned with the magnetic field. The number of pulses is equal to 10, following which the source ‘turns off’. The source produces a channel with a low density and a higher C_s value in comparison with the background. The channel lengthens and its radius remains constant. There forms a preferred direction for the propagation of the source plasma, the AQW, and the MQW.

In the source plasma–background interaction the MQWs are generated in the following way. The plasma expands, forces out the magnetic field and produces a cavern. Electric current flows at the cavern boundary. The magnetic force $\mathbf{J} \times \mathbf{B}$ is directed into the cavern interior and decelerates the source plasma. The same force acts on the background plasma and sets it in motion, which may be compared with the elastic ‘recoil’ of the background. Subsequently the background plasma moves to the cavern centre and compresses about the symmetry axis, which leads to a pressure increase and the plasma outflow along the magnetic field. In the periodic process there forms a narrow ($\sim R_d$) lengthy MQW, at the centre of which the magnetic field is reduced, with a circular current J_ϕ flowing at its boundary. The total pressure in the MQW is equal to the background pressure, which leads to a weak wave attenuation. At the initial stage the MQW velocity exceeds the ion sound

velocity by about a factor of 1.5. Away from the source the MQW velocity is close to the velocity C_s .

The source frequencies ranging from 0.1 to 1 are optimal for producing a lengthy MQW (see Fig. 1). At lower frequencies ($\omega = 0.03$) the modulation of the MQW strengthens and separate waves are formed. For $\omega > 1$ the MQW length depends slightly on the expenditure of energy. The SWMM advantage reveals itself for a large number of pulses and a frequency in the 0.1–1 range, when the lengths of MQWs and AQWs are much greater and the attenuation is weaker than for waves originating from a high-energy pulse.

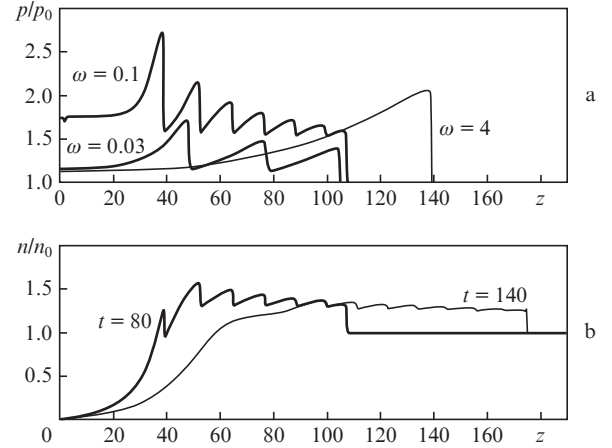


Figure 1. Distributions (on the MQW axis) of the pressure p for different source frequencies ω (a) and of the density n for $\omega = 0.1, t = 80$ and 140 (b). The time is normalised to R_d/C_s and the frequency ω to C_s/R_d . $M_s = 33, M_A = 3.3, L_{pi} = 10$.

Figures 2 and 3 show the influence of ω on the AQW structure. The AQW travels ahead of the MQW at a velocity $C_A \gg C_s$. The optimal frequencies for the AQW production also lie in the 0.1–1 range. For $\omega < 0.1$ the SWMM operates poorly, and in the $\omega > 1$ range the AQW shortens. The respective AQW and MQW radii amount to $\sim 0.5R_d$ and $\sim R_d$. The MQW is a perturbation of the density, pressure, as well as of

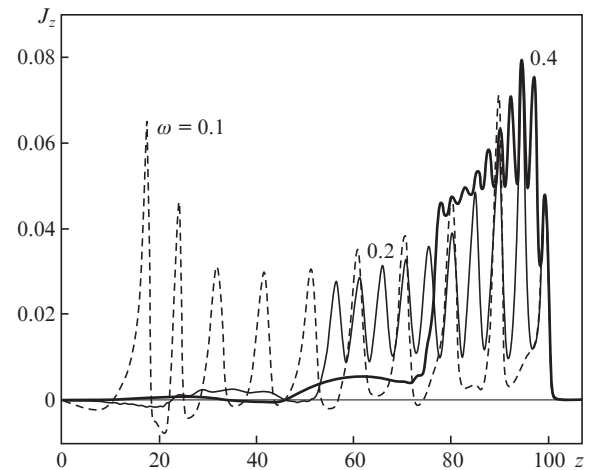


Figure 2. Current distributions on the AQW axis for different ω and $t = 100$. The time is normalised to R_d/C_A and the frequency – to its inverse quantity.

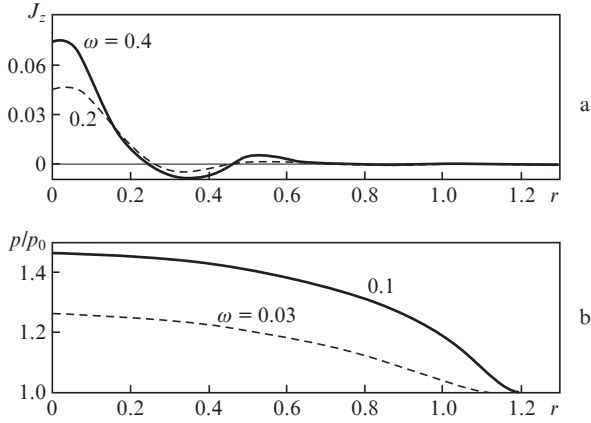


Figure 3. Radial profiles of the current J_z for frequencies $\omega = 0.2$ and 0.4 (a) and of the pressure in a MQW for frequencies $\omega = 0.03$ and 0.1 (b); $t = 100$ and $z = 100$.

the z - and r -components of the plasma velocity and magnetic field. In the AQW there occur torsional rotations of the background plasma about the symmetry z axis, which lead to the torsion of magnetic field lines. The main components are the φ -components of the plasma velocity, magnetic field and current ($J_z \sim \partial B_\varphi / \partial r + B_\varphi / r$), while the perturbations of the density, the z - and r -components of the velocity and field are close to zero. The dimensionless quantities V_φ and B_φ are equal. The Alfvén nature of the AQW is confirmed by Fig. 4. The source produces the MQW and the fast AQW. The V_z velocity is higher than V_φ in the MQW domain and much lower in the AQW domain.

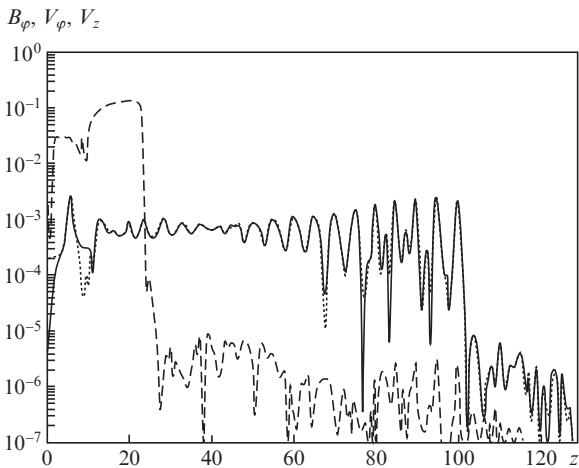


Figure 4. B_φ -component of the field (solid line) as well as the V_φ - (dotted line) and V_z - (dashed line) components of the background plasma velocity at a distance $r = 0.4$ from the z axis plotted along the z axis for $t = 100$ and $\omega = 0.2$.

Figure 5 shows the effect of the initial velocity $M_A = V_0 / C_A$ of source plasma expansion on the amplitude of the longitudinal current on the AQW axis and the source-to-MQW energy conversion efficiency E . The current J_z and other AQW parameters are maximal for $M_A \approx 0.5$. The total efficiency $E = E_s + E_f$ is equal to the ratio between the MQW energy (the thermal and kinetic energy of background and source particles) and the total energy of source pulses (E_s

and E_f are the source and background plasma energy fractions). For $M_A < 1$ the MQW contains the background and source particles, while for $M_A > 1$ only the background particles. In our simulations the ion plasma length far exceeded the dynamic radius ($L_{pi} = 10R_d$). That is why, with the exception of the $M_A \leq 0.1$ domain, the Larmor radius $R_L = M_A L_{pi}$ of source ions also exceeded R_d .

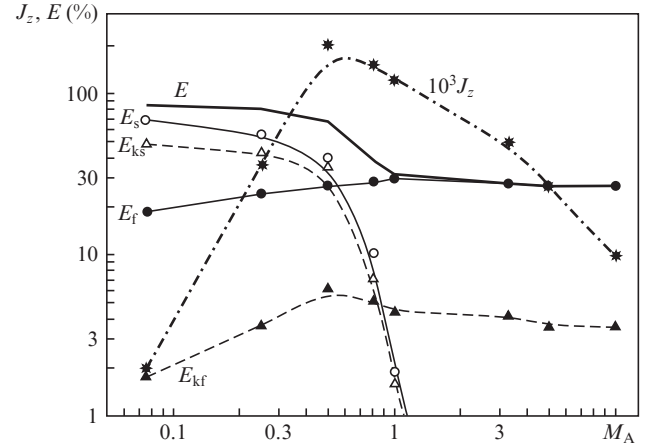


Figure 5. Longitudinal AQW current J_z and total source-to-MQW conversion efficiency $E = E_s + E_f$ as functions of source plasma expansion velocity M_A .

There are two source–background interaction modes – the sub- and super-Alfvénian ones. For $M_A < 1$, the background plasma mass in a volume of radius R_d is small and has no effect on the source plasma at the initial stage of its expansion. The plasma expands to a radius $\sim R_d$, produces a magnetic cavern of the same size, is decelerated by the magnetic field, and subsequently spreads along the field with a velocity $\sim V_0$. In the periodic process the source plasma fills the magnetic field tube. The density becomes equal to the background plasma density in a length $l \sim R_d / M_A^2$. The background density will therefore exceed the source plasma density in the MQW provided the pulse repetition frequency is not too high: $\omega < (R_d / C_A) V_0 / l = M_A^3$. When the Larmor radius is comparable with (or shorter than) the dynamic radius ($R_L = M_A L_{pi} < R_d$), the source and background plasmas are ‘coupled’ due to magnetic laminar mechanism and travel as a whole transversely to the magnetic field. The background plasma is ‘raked up’ and compressed beyond the cavern and spreads along the magnetic field lines, leading to MQW generation. As a result, the source plasma travels jointly with the MQW, which provides a high energy conversion efficiency.

For $M_A > 1$ the source ions are not magnetised ($L_{pi} \gg R_d$) and are slowly decelerated by the field. The magnetic cavern scale length is equal to the distance at which the source plasma density becomes equal to the background density [9]: $R_B \sim R_d / M_A^{2/3}$ and $R_B \ll R_d \ll R_L$. Within the cavern ($r \leq R_B$) the magnetic force $\mathbf{J} \times \mathbf{B}$ accelerates the background ions to the centre (towards the z axis), resulting in the generation of a lengthy MQW, as discussed in the foregoing. The efficiency of MQW generation depends on the length L_{pi} and velocity M_A .

In gases the SWMM forms a QW for $V_0 > C_0$. For a magnetised plasma this requirement is not rigorous. MQW simulations for expansion velocities $M_A < 0.1$ correspond to the subsonic case ($M_s < 1$). Each next pulse catches up with

the MQW due to the high sound velocity in the channel. A steep leading MQW edge is formed at a distance of $\sim (20-30)R_d$ from the source.

In summary we note that the wave merging mechanism operates for all wave types both for a weak and for strong interaction of a pulsating plasma source with the background. The source generates two narrow waves propagating along the magnetic field – the Alfvén wave and the slow magnetosonic one, which contains a substantial fraction of the energy source. The wave radius depends on the energy of individual pulses; the lengths of the waves are proportional to the number of pulses and may far exceed the radius. The attenuation of the waves is weak; their structure may be controlled by varying the pulse repetition frequency and the number of pulses.

Acknowledgements. This work was supported by the Siberian Branch of the Russian Academy of Sciences (SB RAS) (Project No. 113), the Russian Foundation for Basic Research (Grant No. 12-08-00587-a), as well as by Programme No. 22 of the Presidium of the RAS. Our simulations were carried out at the Siberian Supercomputer Centre of the SB RAS.

The authors express their appreciation to A.G. Ponomarenko and Yu.P. Zakharov for helpful discussions, and to N. Yakunkin for his aid in the development of computer programme.

References

1. Tishchenko V.N. *Kvantovaya Elektron.*, **33**, 823 (2003) [*Quantum Electron.*, **33**, 823 (2003)].
2. Tishchenko V.N., Apollonov V.V., Grachev G.N., Gulidov A.I., Zapryagaev V.I., Men'shikov Ya.G., Smirnov A.L., Sobolev A.V. *Kvantovaya Elektron.*, **34**, 941 (2004) [*Quantum Electron.*, **34**, 941 (2004)].
3. Grachev G.N., Ponomarenko A.G., Tishchenko V.N., Smirnov A.L., Trashkeev S.I., Statsenko P.A., Zimin M.I., Myakushina A.A., Zapryagaev V.I., Gulidov A.I., Boiko V.M., Pavlov A.A., Sobolev A.V. *Kvantovaya Elektron.*, **36**, 470 (2006) [*Quantum Electron.*, **36**, 470 (2006)].
4. Tishchenko V.N., Ponomarenko A.G., Posukh V.G., Gulidov A.I., Zapryagaev V.I., Pavlov A.A., Boyarintsev E.L., Golubev M.P., Kavun I.N., Melekhov A.V., Miroshnichenko I.B., Pavlov A.I., Shmakov A.S. *Kvantovaya Elektron.*, **41**, 895 (2011) [*Quantum Electron.*, **41**, 895 (2011)].
5. Tishchenko V.N., Shaikhislamov I.F. *Kvantovaya Elektron.*, **36**, 56 (2006) [*Quantum Electron.*, **36**, 56 (2006)].
6. Tishchenko V.N., Shaikhislamov I.F. *Kvantovaya Elektron.*, **40**, 464 (2010) [*Quantum Electron.*, **40**, 464 (2010)].
7. Akhiezer A.I. (Ed.) *Plasma Electrodynamics* (Oxford: Pergamon Press, 1975; Moscow: Nauka, 1974).
8. Priest E.R. *Solar Magnetohydrodynamics* (Dordrecht: Reidel, 1982; Moscow: Mir, 1985).
9. Zakharov Yu.P., Orishich A.M., Ponomarenko A.G., Posukh V.G. *Fiz. Plazmy*, **12**, 1170 (1986).